Human Molecular Genetics, 2008, Vol. 17, No. 16 **2518–2523**
doi:10.1093/hmg/ddn152
Advance Access published on May 16, 2008

A regulatory SNP of the *BICD1* gene contributes to telomere length variation in humans

Massimo Mangino[1], Scott Brouilette[1], Peter Braund[1], Nighat Tirmizi[1], Mariuca Vasa-Nicotera[1], John R. Thompson[2] and Nilesh J. Samani[1,*]

[1]Department of Cardiovascular Sciences and [2]Department of Health Sciences, University of Leicester, Leicester, UK

Received March 13, 2008; Revised April 27, 2008; Accepted May 14, 2008

Telomeres are repetitive sequences of variable length at the ends of chromosomes involved in maintaining their integrity. Telomere dysfunction is associated with increased risk of cancer and other age-related diseases. Telomere length is an important determinant of telomere function and has a strong genetic basis. We previously carried out a genome-wide linkage analysis of mean leukocyte telomere length, and identified a 12 cM quantitative-trait locus affecting telomere length on human chromosome 12. In the present study we confirmed linkage to this locus in an extended sample (380 families, 520 sib-pairs, maximum LOD score 4.3). Fine-mapping identified a 51 kb region of association within intron 1 of the Bicaudal-D homolog 1 (*BICD1*, MIM 602204) gene. The strongest association ($P = 1.9 \times 10^{-5}$) was with SNP rs2630578 where the minor allele C (frequency 0.21) was associated with telomeres that were shorter by 604 (± 204) base pairs, equivalent to $\sim$15–20 years of age-related attrition in telomere length. Subjects carrying the C allele for rs2630778 had 44% lower *BICD1* mRNA levels in their leukocytes compared with GG homozygotes ($P = 0.004$). BICD1 is involved in Golgi-to-endoplasmic reticulum vacuolar transport. Previous studies have implicated vacuolar genes in telomere length homeostasis in yeast. Our study indicates that *BICD1* plays a similar role in humans.

INTRODUCTION

Telomeres are repetitive DNA-protein structures localized at the ends of chromosomes and specialized in maintaining their integrity. Since the ends of linear chromosomes can only be partially replicated by DNA polymerase (1), telomere maintenance requires the activity of a specialized enzymatic complex, known as telomerase. Telomerase contains both a highly conserved reverse transcriptase (hTERT) and a RNA component (TERC) that provides the template for the telomeric repeats to be synthesized (2). Telomerase is mainly active in germline and proliferating tumour cells (3). As a consequence, telomere length declines with age in all somatic tissues. When telomeres reach a critical length, chromosomal instability and a consequential loss of cell viability ensue (4). Telomere shortening, therefore, has been proposed to be the 'mitotic clock' that regulates cellular lifespan. Support for this hypothesis comes from a number of studies that have examined telomere length as a function of cellular age (5).

The impact of short telomeres on the organism has been studied using a telomerase-deficient mouse model (6). Mice with shorter telomeres showed an increased incidence of tumours, indicating that telomere shortening may increase cancer risk (7). Shorter telomeres have also been associated with a number of human diseases linked to ageing, such as coronary atherosclerosis and myocardial infarction (8,9), heart failure (10), ulcerative colitis (11), and liver cirrhosis (12), as well as several premature ageing syndromes and cancer (3).

Wide inter-individual variation in telomere length exists at birth (13,14) and at any subsequent age (8,15). Twin studies and intra-familial correlation analysis have identified a strong genetic influence on telomere length with up to 80% being genetically determined (16,17). A quantitative-trait locus (QTL) influencing telomere length in mice has been mapped to chromosome 2 (18) with a DNA-helicase like gene, the regulator of telomere length (Rtel) gene, being the most likely cause of the effect (19).

We previously reported a QTL on chromosome 12 influencing telomere length in humans and accounting for up to 50% of the inter-individual variation (20). In the present study we performed linkage and association analyses of an expanded

*To whom correspondence should be addressed at: Department of Cardiovascular Sciences, University of Leicester, Clinical Sciences Wing, Glenfield Hospital, Groby Road, Leicester LE3 9QP, UK. Tel: +44 1162563021; Fax: +44 1162875792. Email: njs@le.ac.uk

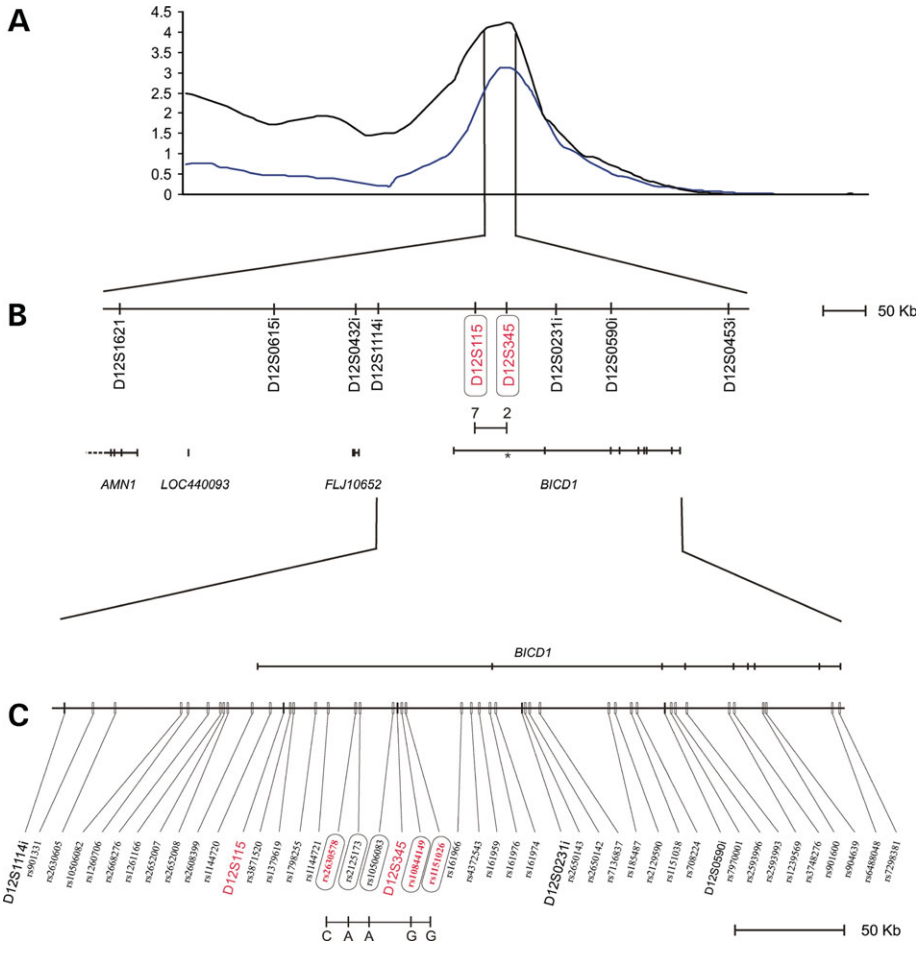

Figure 1. Linkage and association analysis of telomere length with a locus on chromosome 12. (**A**) Shows the results of the linkage analysis. Microsatellite markers are shown on the *x*-axis and LOD score on the *y*-axis. Original quantitative-trait locus (QTL) analysis [from Vasa-Nicotera *et al*. (20)] is represented in blue. QTL analysis of the expanded data set is shown in black. (**B**) Shows the location of nine microsatellite markers analysed to initially refine the chromosome 12 locus through association analysis, and also provides annotation of the genes within the region. *AMN1*, antagonist of mitotic exit network 1; *LOC440093*, histone H3-like; *FLJ6052*, chromosome 12 open reading frame 35; *BICD1*, Bicaudal-D homolog 1. The analysis identified a significant association with telomere length for specific alleles of markers D12S345 and D12S115 (in red). Two-marker sliding-window approach revealed a haplotype 7_2 of these microsatellites associated with telomere length variation, which is shown. The asterisk indicates the position of D12S345 relative to *BICD1* gene. (**C**) Shows the location in relation to *BICD1* of the 40 SNPs analysed for association in relation to BICD1. The relative positions of the microsatellites described in Figure 2B are also shown in red. Haplotype analysis identified one haplotype (CAAGG) derived from five SNPs (shown in boxes) that showed a significant association with telomere length. A scale in kb is shown for (B) and (C).

data set with a view to identifying the gene(s) and variants that underlie the QTL on chromosome 12.

RESULTS

We initially expanded our previous linkage analysis in 177 families ($n = 229$ sib-pairs) (20), by measuring telomere lengths in a further 203 families ($n = 291$ sib-pairs) from the British Heart Foundation Family Heart Study (BHF-FHS) (21). The total number of subjects was 843 (72% males) with a mean age of 61.8 $\pm$ 7.0 years (Supplementary Material, Table S1). The expanded analysis supported our previous finding of linkage of telomere length with a locus on chromosome 12p11.2-q12 with the LOD score at the peak marker, D12S345, increasing from 3.2 to 4.3 (Fig. 1A).

Having confirmed linkage to chromosome 12, we used family-based association tests (FBAT) to examine the association of microsatellites in the region underlying the linkage peak with telomere length. Analysis of the full study population showed a significant association with a specific allele (allele 2) of marker D12S345 ($P = 5.6 \times 10^{-4}$). We then focused on a $\sim$700 kb region centred on the marker D12S345 and typed an additional eight microsatellite markers (Fig. 1B). Analysis of these also detected an association between allele 7 of marker D12S115 and telomere length variation ($P = 8.3 \times 10^{-4}$). Similar results were obtained using the quantitative transmission disequilibrium tests (QTDT) software ($P = 0.001$ and 0.02, for D12S345 and D12S115 respectively, after 1000 Monte-Carlo permutations).

Allele 2 of D12S345 and allele 7 of D12S115 were associated with shorter telomeres of 534 $\pm$ 192 (SE) base pairs (bp) and 701 $\pm$ 224 bp, respectively, compared with all the other alleles combined for each microsatellite (Table 1). We also carried out a haplotype analysis on the nine typed microsatellite markers. A 2-markers sliding-window approach revealed

Table 1. Phenotypic effect size of markers associated with telomere restriction fragment (TRF)[a]

Marker	Associated allele	Frequency	FBAT *P*-value*	Effect (SE) in bp
D12S345	2	0.22	5.6×10^{-4}	−534 (±192)
D12S115	7	0.21	8.3×10^{-4}	−701 (±224)
rs2630578	C	0.21	1.9×10^{-5}	−604 (±204)
rs1151026	G	0.21	3.9×10^{-4}	−452 (±182)

[a]Age- and gender-adjusted.
*P-value after 1×10^9 permutations tests.

one haplotype (7_2), formed by the respective alleles for markers D12S115 and D12S345, associated with mean telomere length ($P = 6 \times 10^{-3}$) (Fig. 1B).

According to NCBI (Build 36), the region marked by this haplotype contains only one gene, Bicaudal-D homolog 1 (*BICD1*, MIM 602204). To further investigate the role of this region, and in particular *BICD1*, we analysed a set of 40 Tag-SNPs spanning the ∼360 kb region between D12S1114i (the first not associated microsatellite marker) and including the entire *BICD1* gene (Fig. 1C). After correction for multiple testing (see Materials and Methods), the strongest associated single SNP was rs2630578 ($P = 1.9 \times 10^{-5}$) where the C allele (frequency, 0.21) was associated with telomeres that were shorter by 604 (±204) bp (Table 1). One further SNP (rs1151026) also showed a significant association after allowing for multiple testing (Table 1). Haplotype analysis identified one haplotype (CAAGG, frequency 17%) composed by alleles of five SNPs (rs2630578, rs2125173, rs10506083, rs10844149 and rs1151026) all located within intron 1 of *BICD1* gene that showed positive association with telomere length ($P = 1.3 \times 10^{-4}$) (Fig. 1C).

To further confirm that the associated SNPs are relevant to the observed linkage of telomere length with chromosome 12p, we investigated the covariate effect of the most significant SNP (rs2630578) on the chromosome 12 LOD score value. Inclusion of rs2630578 in the linkage analysis decreased the LOD score from 4.32 to 3.11. Inclusion of all five SNPs of the haplotype gave a similar reduction of the LOD score value (3.15). Because all the sib-pairs analysed had coronary artery disease (CAD, see Materials and Methods), we also examined the linkage and association of the locus with CAD. There was no signal. Notably, D12S345, with a LOD score of 4.32 for telomere length, has a LOD score of 0.00 for CAD.

Given the location of rs2630578 and the associated haplotype within intron 1 of the *BICD1* gene we hypothesized that the functional variants may act by influencing *BICD1* expression levels. To test this hypothesis we designed PCR primers targeting *BICD1*. The forward primer was placed in the exon1–exon2 boundary and the reverse primer on the exon-2 sequence. Both primers were designed to be specific to *BICD1*. Expression of *BICD1* was then measured in leukocytes of healthy adult individuals ($n = 18$) with different genotypes (CC, CG and GG) for rs2630578. Analysis of variance showed a significant difference in steady state *BICD1* mRNA levels between the three genotypes (Fig. 2, $P = 0.014$). Individual comparisons (Bonferroni adjusted) between the genotypes gave *P*-values of GG versus CC 0.016, GG versus CG 0.071 and CG versus CC 1.000, suggesting a dominant

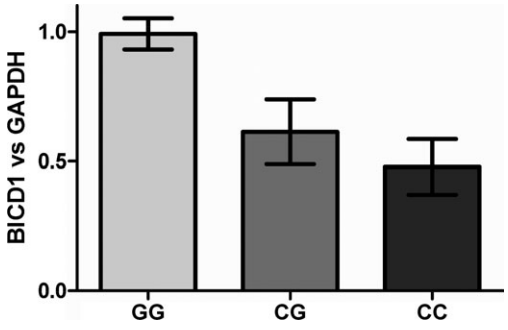

Figure 2. Relative *BICD1* mRNA levels in leukocytes of healthy subjects with different rs2630578 genotypes. Data are mean (±SD) of relative mRNA levels ($n = 6$ per genotype group).

effect of the C allele. Under this model, subjects carrying the C allele for rs2630578 had 44% (95% CI: 16–72%) lower *BICD1* mRNA levels compared with GG homozygotes ($P = 0.004$).

DISCUSSION

Our previous genome-wide analysis identified a 12 cM locus on chromosome 12 influencing telomere length in human (20). In this study, we provide further evidence of linkage of this locus with telomere length and identify variants within intron 1 of the *BICD1* gene that are significantly associated with telomere length. The findings identify *BICD1* as a novel regulator of telomere length in humans. This is the first demonstration of a specific gene regulating telomere length in humans.

As in the previous study (20), we measured telomere restriction fragment (TRF) length in sib-pair with CAD. This was done for pragmatic reasons as the cohort already had genotype data available from a linkage scan of 400 microsatellite markers (21). Given the evidence linking shorter telomeres with risk of CAD (8,22), it was first important to rule out the possibility that our results are spurious and related to an association of the locus with CAD. We therefore performed both linkage and association analysis in the complete data set using CAD as phenotype. The results showed no statistically significant *P*-value at any of the markers analysed in this study. We conclude that our results are unlikely to reflect linkage or association with CAD. However, further studies in other cohorts, and in particular subjects without CAD, are required to establish the generalizability of our findings.

Although this is the first time that a protein involved in the vacuolar traffic has been associated with telomere length maintenance in humans, a number of yeast studies already provide substantial evidence of a link between vacuolar genes and shorter telomeres (23–25). In a genome-wide screen for *Saccharomices Cerevisiae* deletion mutants, Askree *et al*. (23) identified 173 new candidates genes that affect telomere length. Of these, 30 are involved in vacuolar traffic. A subsequent study to investigate the link between vacuolar traffic and telomere length maintenance suggested that vacuolar genes probably regulate telomere length by effects on the telomerase and Ku pathways (25). In this context, our finding that the same allele of SNP rs2630578 (allele C) that is associated with shorter telomeres is also associated with significantly lower steady-state *BICD1* mRNA level in leukocytes may be relevant. Lower expression

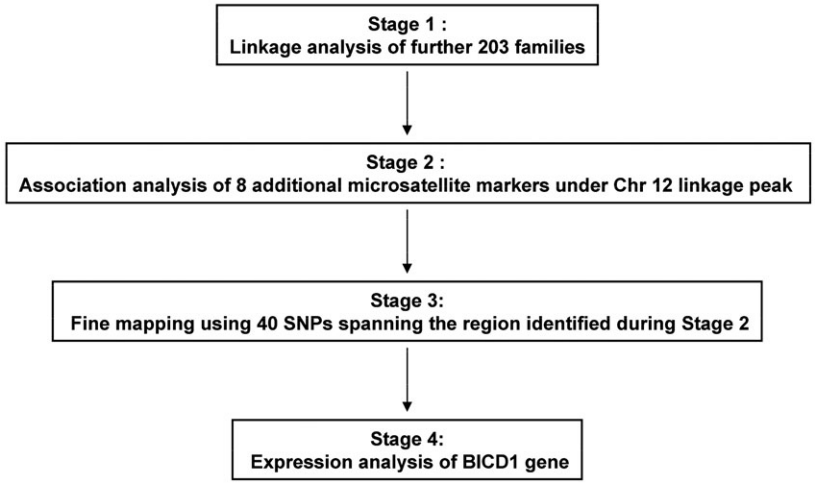

Figure 3. Schematic of the experimental design and stages.

of this allele could affect the amount of BICD1 available for vacuolar trafficking, which in turn may influence telomere maintenance.

The associated polymorphism rs2630578 lies in a block of highly conserved sequence. Evolutionary sequence conservation is believed to indicate regions of biological function (26) and SNPs in non-coding sequences, such as enhancers, repressors or chromatin structural regulators, might play a fundamental role in disease risk by modulating transcriptional levels for key genes (27). In this regard, we hypothesized that rs2630578 SNP could affect a transcription factor binding site within one such regulatory element. Interestingly, the region surrounding rs2630578 demonstrates trimethylation of Histone 3 at lysine 4 (H3K4 me3), an epigenetic hallmark of enhancers. A further analysis with R-vista (v2.0) (28), also showed that the C allele of rs2630578 disrupts a putative sequence for a Nuclear Factor Y (NF-Y) transcription factor. Of note, a number of studies have demonstrated that attenuation or suppression of the NF-Y function leads to cellular ageing (29). Moreover, a recent study showed that NF-Y removal resulted in a decrease in transcription of expressed genes associated with H3K4me3 (30). This observation would be consistent with our experimental data, and suggest that rs2630578 allele C may lead to a reduction in *BICD1* expression and relative telomere length shortening via disruption of NF-Y factor binding.

Several studies have shown an age-related attrition rate of telomere length in leukocytes between 25 and 35 bp per year (8,15,16,20,31). Viewed from this perspective, the effect of the *BICDI* gene variants on telomere length (Table 1) is substantial, as it is equivalent to between 15 and 20 years of age-related attrition in telomere length. Given the role of telomere length in various age-related diseases (5), it will be interesting to examine whether there is an association of the locus with susceptibility to some of these diseases, although it is notable that despite the evidence of an association of shorter telomeres with increased risk of CAD (8,22), we did not see an association of the locus with CAD.

Inclusion of the most significant SNP in *BICD1* associated with telomere length (rs2630578) as a covariate in the linkage analysis reduced the LOD score by 28% confirming that it is a major contributor to the observed linkage. However, the finding that it does not completely explain the linkage peak, suggests that other genes and variants could play a role. Therefore, further analysis of the locus, perhaps through a more extensive association analysis is warranted. Notwithstanding this, through a sequential fine mapping strategy of a linkage peak, we report identification of a gene involved in the vacuolar traffic regulating telomere length in humans.

MATERIALS AND METHODS

The flow of work is described in Figure 3.

Expansion of linkage analysis for telomere length

Families used to expand the linkage analysis were, as per the previous study (20), randomly chosen from those participating in the BHF-FHS (21) and consisted of sib-pairs both with CAD. Further details of the families are described in Supplementary Material, Table S1. White cell mean telomere lengths were measured using Southern blotting as previously described (8,20). Data were available on all subjects from a previous linkage scan of 400 microsatellite markers from the ABI-Prism Linkage Mapping set v2.5-MD10 (PE Applied Biosystems), spaced at $\sim$10 cM and with an average heterozygosity of 0.79 (21).

Fine mapping of chromosome 12 locus

To refine the chromosome 12 locus, initially an additional eight microsatellite markers spanning a region of $\sim$700 kb around the marker D12S345 were genotyped (Fig. 1B). Markers *D12S0619i, D12S0615i, D12S0432i, D12S1114i, D12S0231i, D12S0590i* and *D12S0435i* were selected from the gene diversity database system (GDBS). Marker D12S115 was identified

from a predicted tandem repeat region in the GDBS database. Subsequently, 40 Tag-SNPs (minor allele frequency (MAF) > 5%) were selected with the SNPbrowser software (V3.1; Applied Biosystems), using linkage disequilibrium (LD) database from HapMap (NCBI Build 35) and the Haplotype R^2 method. The location and characteristics of all the SNPs are shown in Supplementary Material, Table S2 and Figure 1C. Genotyping of the SNPs was undertaken using the SNPlex^{TM} Genotyping System (Applied Biosystems). The SNP-specific ligation probes were designed on-demand by Applied Biosystems. All the steps of the SNPlex^{TM} assay workflow (allele-specific oligonucleotide ligation assay (OLA) reaction; OLA purification; PCR; hybridization of PCR products to ZipChute Probes, elution and electrophoresis) were performed according to the manufacturer protocol. The electrophoretic runs were analysed on a 3130*xl* DNA Analyser (Applied Biosystems). GeneMapper® software (V. 3.7; Applied Biosystems) was used to analyse the raw data and to call SNPs genotypes. All genotypes (microsatellite markers and SNPs) were confirmed by visual inspection of chromatograms. Inheritance within families was verified using the PEDCHECK program (32). In case of possible inheritance errors, the complete family was genotyped again and if the discrepancy could not be resolved then the family for that marker was excluded.

Expression analysis of *BICD1*

Six subjects for each rs2630578 genotype were identified by genotyping 338 individuals from a population-based cohort recruited for genetic studies. Characteristics of this cohort are described elsewhere (33). All subjects chosen (nine males, nine females, mean age 39.4 ± 3.5 years) were healthy and not on any medication. Total RNA was extracted from blood leukocytes using the Mini RNeasy Total RNA isolation kit (Qiagen), and the concentration and purity of RNA was determined using a ND-1000 spectrophotometer (NanoDrop). First-strand cDNA synthesis was performed using SuperScript^{TM} III (Invitrogen) and oligo(dT)$_{12-18}$ (Invitrogen) according to the manufacturer's instructions. Q-PCR was then performed in triplicate for each sample using a 7900HT instrument (Applied Biosystems) and SYBR® Green PCR master mix (Applied Biosystems). The primer sequences used were 5′-CCTCAAACAGCAGTATGATGAAC-3′ and 5′-CAAAT GCCTCTTTGAGCTG-3′. Thermal cycle parameters were as follows: 95°C for 10 min, 40 cycles of denaturation at 95°C for 45 s, annealing at 59°C for 45 s and extension at 72°C for 45 s. Dissociation curves were generated by denaturation at 95°C for 15 s and annealing at 60°C for 15 s followed by a gradual increase in temperature (2% ramp rate) to 95°C. Standard curves were generated for each primer pair with serial dilutions of cDNA. Melting curve analysis was used to assess PCR specificity. The Ct of the target gene (*BICD1*) was normalized to that of the reference gene (*GAPDH*). In the relative quantification approach used, the efficiency corrected quantification model as described by Pfaffl (34), was applied.

Statistical analysis

For the expanded linkage analysis, two-point and multipoint quantitative-trait linkage analysis was performed with the sequential oligogenic linkage analysis routines (SOLAR) package (version 1.7.3) (35). The analysis was carried out using gender and age as covariates. Allele frequencies were calculated using the observed genotypes. The order of the marker loci and the recombination distances used for multipoint linkage analysis were based on the deCODE map (36).

Association analyses for both microsatellite markers and SNPs were carried out using the FBAT software (V. 1.7.3) (37) after prior adjustment for age and sex. For these analyses we used the empirical correction to the variance (option-e) (38) because we tested multiple sibs families under the null hypothesis of 'linkage, but not association'. The exact *P*-values were calculated using the option '-p' and 1×10^9 Monte Carlo simulations.

Haplotype analysis was carried out using the HBAT command of FBAT. The '-e' and '-p' options were used for this analysis also. The results of FBAT analysis were validated using the orthogonal model (39) implemented in QTDT software (40), including gender and age as covariates. In order to calculate a global *P*-value adjusted for multiple testing, we used the '-m' option to calculate 1000 Monte-Carlo permutations.

In the SNP association analysis, to control for multiple testing, we used a SNP spectral decomposition method proposed by Nyholt (41) and modified by Li and Ji (42). The correction was based on the spectral decomposition of matrices of pair wise LD between SNPs and calculation of the effective number of independent genetic marker loci along with the significance threshold required to keep the type I error rate at 5%. The SNP spectral decomposition approach is preferred to be a more conservative correction which does not account for LD-driven dependence among markers and thus may overestimate the level of type I error and reduce the power to detect associations. After spectral decomposition of the LD matrices of the 40 analysed SNPs, the corrected threshold of statistical significance in the single-locus association study was estimated at $P \leq 0.002$.

The phenotypic effect size of significant SNPs was calculated using general estimating equations. This method uses all available information of the analysed families, including the uninformative pedigrees, which do not contribute to the FBAT statistics (43). This option is available in the PBAT (44) package (option 4 of the estimate effect size analysis tool).

Relative *BICD1* mRNA levels were compared in subjects carrying different rs2630578 genotypes using analysis of variance and Student's *t*-test.

SUPPLEMENTARY MATERIAL

Supplementary Material is available at HMG Online.

Conflict of Interest statement. None declared.

FUNDING

We are grateful to the British Heart Foundation (BHF) for supporting this work. N.J.S. holds a BHF Chair in Cardiology.

REFERENCES

1. Olovnikov, A.M. (1973) A theory of marginotomy. The incomplete copying of template margin in enzymic synthesis of polynucleotides and biological significance of the phenomenon. *J. Theor. Biol.*, **41**, 181–190.
2. Blackburn, E.H. (2001) Switching and signaling at the telomere. *Cell*, **106**, 661–673.
3. Callen, E. and Surralles, J. (2004) Telomere dysfunction in genome instability syndromes. *Mutat. Res.*, **567**, 85–104.
4. Collins, K. and Mitchell, J.R. (2002) Telomerase in the human organism. *Oncogene*, **21**, 564–579.
5. Blasco, M.A. (2007) The epigenetic regulation of mammalian telomeres. *Nat. Rev. Genet.*, **8**, 299–309.
6. Blasco, M.A. (2005) Mice with bad ends: mouse models for the study of telomeres and telomerase in cancer and aging. *EMBO J.*, **24**, 1095–1103.
7. Rudolph, K.L., Chang, S., Lee, H.W., Blasco, M., Gottlieb, G.J., Greider, C. and DePinho, R.A. (1999) Longevity, stress response, and cancer in aging telomerase-deficient mice. *Cell*, **96**, 701–712.
8. Brouilette, S., Singh, R.K., Thompson, J.R., Goodall, A.H. and Samani, N.J. (2003) White cell telomere length and risk of premature myocardial infarction. *Arterioscler. Thromb. Vasc. Biol.*, **23**, 842–846.
9. Nakashima, H., Ozono, R., Suyama, C., Sueda, T., Kambe, M. and Oshima, T. (2004) Telomere attrition in white blood cell correlating with cardiovascular damage. *Hypertens. Res.*, **27**, 319–325.
10. Oh, H., Wang, S.C., Prahash, A., Sano, M., Moravec, C.S., Taffet, G.E., Michael, L.H., Youker, K.A., Entman, M.L. and Schneider, M.D. (2003) Telomere attrition and Chk2 activation in human heart failure. *Proc. Natl Acad. Sci. USA*, **100**, 5378–5383.
11. O'Sullivan, J.N., Bronner, M.P., Brentnall, T.A., Finley, J.C., Shen, W.T., Emerson, S., Emond, M.J., Gollahon, K.A., Moskovitz, A.H., Crispin, D.A. *et al.* (2002) Chromosomal instability in ulcerative colitis is related to telomere shortening. *Nat. Genet.*, **32**, 280–284.
12. Wiemann, S.U., Satyanarayana, A., Tsahuridu, M., Tillmann, H.L., Zender, L., Klempnauer, J., Flemming, P., Franco, S., Blasco, M.A., Manns, M.P. *et al.* (2002) Hepatocyte telomere shortening and senescence are general markers of human liver cirrhosis. *FASEB J.*, **16**, 935–942.
13. Akkad, A., Hastings, R., Konje, J.C., Bell, S.C., Thurston, H. and Williams, B. (2006) Telomere length in small-for-gestational-age babies. *BJOG*, **113**, 318–323.
14. Okuda, K., Bardeguez, A., Gardner, J.P., Rodriguez, P., Ganesh, V., Kimura, M., Skurnick, J., Awad, G. and Aviv, A. (2002) Telomere length in the newborn. *Pediatr. Res.*, **52**, 377–381.
15. Slagboom, P.E., Droog, S. and Boomsma, D.I. (1994) Genetic determination of telomere size in humans: a twin study of three age groups. *Am. J. Hum. Genet.*, **55**, 876–882.
16. Andrew, T., Aviv, A., Falchi, M., Surdulescu, G.L., Gardner, J.P., Lu, X., Kimura, M., Kato, B.S., Valdes, A.M. and Spector, T.D. (2006) Mapping genetic loci that determine leukocyte telomere length in a large sample of unselected female sibling pairs. *Am. J. Hum. Genet.*, **78**, 480–486.
17. Jeanclos, E., Schork, N.J., Kyvik, K.O., Kimura, M., Skurnick, J.H. and Aviv, A. (2000) Telomere length inversely correlates with pulse pressure and is highly familial. *Hypertension*, **36**, 195–200.
18. Zhu, L., Hathcock, K.S., Hande, P., Lansdorp, P.M., Seldin, M.F. and Hodes, R.J. (1998) Telomere length regulation in mice is linked to a novel chromosome locus. *Proc. Natl Acad. Sci. USA*, **95**, 8648–8653.
19. Ding, H., Schertzer, M., Wu, X., Gertsenstein, M., Selig, S., Kammori, M., Pourvali, R., Poon, S., Vulto, I., Chavez, E. *et al.* (2004) Regulation of murine telomere length by Rtel: an essential gene encoding a helicase-like protein. *Cell*, **117**, 873–886.
20. Vasa-Nicotera, M., Brouilette, S., Mangino, M., Thompson, J.R., Braund, P., Clemitson, J.R., Mason, A., Bodycote, C.L., Raleigh, S.M., Louis, E. *et al.* (2004) Mapping of a major locus that determines telomere length in humans. *Am. J. Hum. Genet.*, **76**, 147–151.
21. BHF Family Heart Study Research Group (2005) A Genomewide linkage study of 1,933 families affected by premature coronary artery disease: The British Heart Foundation (BHF) Family Heart Study. *Am. J. Hum. Genet.*, **77**, 1011–1020.
22. Cawthon, R.M., Smith, K.R., O'Brien, E., Sivatchenko, A. and Kerber, R.A. (2003) Association between telomere length in blood and mortality in people aged 60 years or older. *Lancet*, **361**, 393–395.
23. Askree, S.H., Yehuda, T., Smolikov, S., Gurevich, R., Hawk, J., Coker, C., Krauskopf, A., Kupiec, M. and McEachern, M.J. (2004) A genome-wide screen for Saccharomyces cerevisiae deletion mutants that affect telomere length. *Proc. Natl Acad. Sci. USA*, **101**, 8658–8663.
24. Gatbonton, T., Imbesi, M., Nelson, M., Akey, J.M., Ruderfer, D.M., Kruglyak, L., Simon, J.A. and Bedalov, A. (2006) Telomere length as a quantitative trait: genome-wide survey and genetic mapping of telomere length-control genes in yeast. *PLoS Genet.*, **2**, e35.
25. Rog, O., Smolikov, S., Krauskopf, A. and Kupiec, M. (2005) The yeast VPS genes affect telomere length regulation. *Curr. Genet.*, **47**, 18–28.
26. Hardison, R.C. (2000) Conserved noncoding sequences are reliable guides to regulatory elements. *Trends Genet.*, **16**, 369–372.
27. Emison, E.S., McCallion, A.S., Kashuk, C.S., Bush, R.T., Grice, E., Lin, S., Portnoy, M.E., Cutler, D.J., Green, E.D. and Chakravarti, A. (2005) A common sex-dependent mutation in a RET enhancer underlies Hirschsprung disease risk. *Nature*, **434**, 857–863.
28. Loots, G.G. and Ovcharenko, I. (2004) rVISTA 2.0: evolutionary analysis of transcription factor binding sites. *Nucleic Acids Res.*, **32**, W217–W221.
29. Matuoka, K. and Chen, K.Y. (2002) Transcriptional regulation of cellular ageing by the CCAAT box-binding factor CBF/NF-Y. *Ageing Res. Rev.*, **1**, 639–651.
30. Ceribelli, M., Dolfini, D., Merico, D., Gatta, R., Vigano, A.M., Pavesi, G. and Mantovani, R. (2008) The histone-like NF-Y is a bifunctional transcription factor. *Mol. Cell. Biol.*, **28**, 2047–2058.
31. Benetos, A., Okuda, K., Lajemi, M., Kimura, M., Thomas, F., Skurnick, J., Labat, C., Bean, K. and Aviv, A. (2001) Telomere length as an indicator of biological aging: the gender effect and relation with pulse pressure and pulse wave velocity. *Hypertension*, **37**, 381–385.
32. O'Connell, J.R. and Weeks, D.E. (1998) PedCheck: a program for identification of genotype incompatibilities in linkage analysis. *Am. J. Hum. Genet.*, **63**, 259–266.
33. Tobin, M.D., Raleigh, S.M., Newhouse, S., Braund, P., Bodycote, C., Ogleby, J., Cross, D., Gracey, J., Hayes, S., Smith, T. *et al.* (2005) Association of WNK1 gene polymorphisms and haplotypes with ambulatory blood pressure in the general population. *Circulation*, **112**, 3423–3429.
34. Pfaffl, M.W. (2001) A new mathematical model for relative quantification in real-time RT-PCR. *Nucleic Acids Res.*, **29**, e45.
35. Almasy, L. and Blangero, J. (1998) Multipoint quantitative-trait linkage analysis in general pedigrees. *Am. J. Hum. Genet.*, **62**, 1198–1211.
36. Kong, A., Gudbjartsson, D.F., Sainz, J., Jonsdottir, G.M., Gudjonsson, S.A., Richardsson, B., Sigurdardottir, S., Barnard, J., Hallbeck, B., Masson, G. *et al.* (2002) A high-resolution recombination map of the human genome. *Nat. Genet.*, **31**, 241–247.
37. Horvath, S., Xu, X. and Laird, N.M. (2001) The family based association test method: strategies for studying general genotype–phenotype associations. *Eur. J. Hum. Genet.*, **9**, 301–306.
38. Lake, S.L., Blacker, D. and Laird, N.M. (2000) Family-based tests of association in the presence of linkage. *Am. J. Hum. Genet.*, **67**, 1515–1525.
39. Abecasis, G.R., Cookson, W.O. and Cardon, L.R. (2000) Pedigree tests of transmission disequilibrium. *Eur. J. Hum. Genet.*, **8**, 545–551.
40. Abecasis, G.R., Cardon, L.R. and Cookson, W.O. (2000) A general test of association for quantitative traits in nuclear families. *Am. J. Hum. Genet.*, **66**, 279–292.
41. Nyholt, D.R. (2004) A simple correction for multiple testing for single-nucleotide polymorphisms in linkage disequilibrium with each other. *Am. J. Hum. Genet.*, **74**, 765–769.
42. Li, J. and Ji, L. (2005) Adjusting multiple testing in multilocus analyses using the eigenvalues of a correlation matrix. *Heredity*, **95**, 221–227.
43. Lange, C., DeMeo, D., Silverman, E.K., Weiss, S.T. and Laird, N.M. (2003) Using the noninformative families in family-based association tests: a powerful new testing strategy. *Am. J. Hum. Genet.*, **73**, 801–811.
44. Lange, C., DeMeo, D., Silverman, E.K., Weiss, S.T. and Laird, N.M. (2004) PBAT: tools for family-based association studies. *Am. J. Hum. Genet.*, **74**, 367–369.